# Effect of Glass Surface Roughness on Separation Energy in Low Temperature Ultrasonic Soldering

Mustafa M.Y., Mohamad H. E., Hilmy I., Adesta* E. Y. T.

School of Materials and Manufacturing Engineering, Faculty of Engineering, International Islamic University Malaysia, Kuala Lumpur, Malaysia.

* eadesta@gmail.com

**Abstract.** Giftware products combining pewter (Sn5Sb1.2Cu) and glass require good matching up for strong adhesive bonding. The possibility of joining the parts without good matching using ultrasonic soldering is commercially attractive. Ultrasonic soldering was applied to bond the two substrates using (Sn40Bi)0.5Al as solder alloy at temperature not exceeding 450 °C. All parameters were kept constant except for the glass surface roughness. Analyses were conducted on the effects of glass surface roughness on shear separation force and extension before fracture of solder joint. The separation force and extension before fracture were determined by subjecting the soldered specimen to tensile stress test. Effect on shear separation energy was derived by calculation. Separation energy of joint between glass and Sn5Sb1.2Cu based on ultrasonic soldering can be strengthened by increasing glass surface roughness.

**Keywords:** Ultrasonic solder; glass solder; surface roughness effect; solder separation energy; solder separation force

## 1      Introduction

Giftware products combining pewter (Sn5Sb1.2Cu by weight %) and glass require good matching up for strong adhesive bonding. Gaps in between weaken the adhesive bonding. Ultrasonic soldering (US) combining heat and ultrasonic vibration enables soldering of the two parts with moderate matching up. Molten solder fills the gaps. The possibility of joining the parts without good matching is commercially attractive. US adhesion strength is affected by soldering time and temperature, type of solder alloy, vibrational amplitude and frequency. The effect of surface roughness to joint strength was investigated in this study.

[1, 2] demonstrated the range of optimum soldering time for strong US joint of 2024 Al using Zn-Al and pure Sn filler metals respectively. Higher soldering time strengthened the joint by increasing diffusion of Al and alumina into the filler metals. [3, 4] optimized the relationship between tensile strength and soldering temperature of US 5056 Al joints using Zn-Al and Zn-Sn solder alloys respectively. Solder joint weakened when soldering temperature was above the liquidus point due to intermetallic compound formation. [5] established the range of vibration amplitude for optimum tensile strength in US of 1070 Al using Sn23Zn solder alloy.

Very high vibration amplitude weakened the joint by squeezing out solder alloy from the joint gap. Frequency selection for US varies between substrates and applications. Harder and brittle materials require higher frequency vibrations for stronger bond. Lower frequencies of 19 to 21 kHz were used mostly for bonding metals [3, 4, 5, 6, 7]. Medium level frequency at 40 kHz was used for thermosonic bonding and US of amorphous metals [8, 9, 10]. Higher frequency at 60 kHz was used for glass and ceramics [11].

This research focused on the effects of glass surface roughness on US joint strength between glass and Sn5Sb1.2Cu. Metal oxide adhesion bonded ceramic and metal together [12]. US was conducted using a manually held soldering tool from 'Sunbonder USM-5' US device. Soda-lime-silica flat glass was selected due to its flatness, simplifying measurement of surface roughness and separation force. Sn5Sb1.2Cu was selected due to its commercial usage and low melting temperature. Solder alloy (Sn40Bi)0.5Al by weight % was selected due to its low melting temperature and good adhesion to both glass and Sn5Sb1.2Cu. Analyses were conducted on shear separation force, extension before fracture and shear separation energy. US was conducted at temperature not exceeding 450 °C to reduce damage to glass and Sn5Sb1.2Cu.

## 2    Materials and Methods

The 2 mm thick soda-lime-silica glass panel was cut to dimensions of 33 x 16 x 2 mm. Sn5Sb1.2Cu was melted and cast in steel mold, rolled to 2 mm thick and cut into dimensions of 55 x 20 x 2 mm. (Sn40Bi)0.5Al was cast into 2mm diameter rod and cut at uniform weight of 0.10 gram. Table 1 shows the mechanical properties of Sn5Sb1.2Cu, (Sn40Bi)0.5Al and glass. Table 2 shows the chemical compositions and solidus/ liquidus temperatures of both Sn5Sb1.2Cu and (Sn40Bi)0.5Al.

Soldering was conducted on a fabricated apparatus attached with 150 W electrical heater as schematically shown in Figure 1. Substrate temperature was set at optimum 150 °C. Lower setting inhibited solder flow while higher setting delayed solidification after soldering. Glass surface was wiped clean with petrol and inserted into the apparatus. Two segments of glass surface was roughened by manually rubbing with 'Sunbonder USM-5' soldering tool tip having longitudinal vibration set at 450 °C. Ultrasonic power was set at 2W, 4W, 6W, 8W, 10W and 12W with time duration of 2, 4, 6 and 8 minutes. Observations were made on the vibration amplitude at specific ultrasonic power. After surface roughening, the glass specimen was removed from apparatus for surface roughness measurement using Mitutoyo Surftest and inserted back.

**Table 1**    Mechanical properties of glass, Sn5Sb1.2Cu and (Sn40Bi)0.5Al.

| Material | Tensile strength (MPa) | Elongation % |
|---|---|---|
| Sn5Sb1.2Cu | 39.6 | 8.78 |
| (Sn40Bi)0.5Al | 70.6 | 5.40 |
| Soda Lime Glass | 30 | 0.22 |

**Table 2**    Chemical compositions (by weight %) and solidus ($Ts$) and liquidus ($Tl$) temperatures of Sn5Sb1.2Cu and (Sn40Bi)0.5Al.

| Material | Sn | Bi | Cu | Al | Others | $Ts$ °C | $Tl$ °C |
|---|---|---|---|---|---|---|---|
| Sn5Sb1.2Cu | 93.61 | 5.00 | 1.20 | | Bal. | 222.4 | 236.0 |
| (Sn40Bi)0.5Al | 59.64 | 39.76 | | 0.50 | Bal. | 143.3 | 170.7 |

Sn5Sb1.2Cu specimen was inserted after removal of oxide layer through knife scrapping. At substrates temperature of 150 °C, the 0.10 gram solder granule was placed on glass. Vibrating solder tool at 450 °C melted and spread out the granule to glass surface and the edge of Sn5Sb1.2Cu for 30 seconds per segment. This was repeated on the next segment. The specimen was cooled to room temperature before removal. The measured soldered area for two segments was at 1.12 cm$^2$.
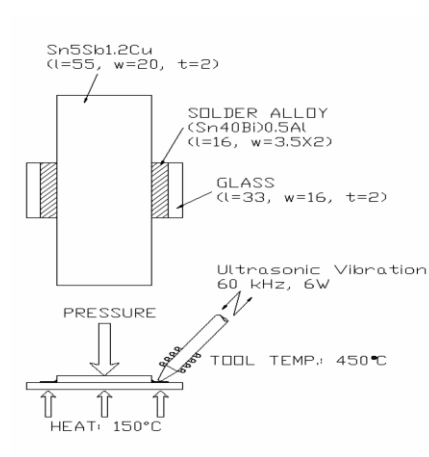


**Figure 1**   Schematic illustration of ultrasonic soldering apparatus
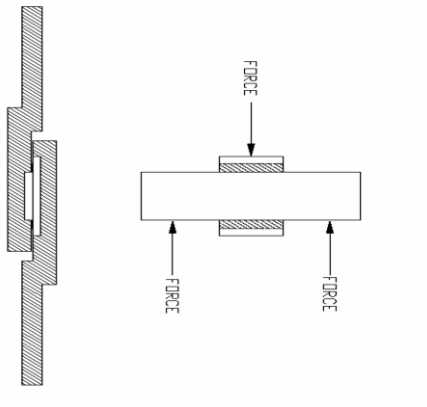
**Figure 2**    Schematic diagram of shear tensile test of glass and Sn5Sb1.2Cu

The soldered specimen was inserted into the tensile test apparatus and subjected to shear tensile test on Instron 5582 tension testing machine as schematically shown in Figure 2. Test was conducted at room temperature and at constant rate of 2 mm/ min. Data collected on shear separation force and extension before fracture was based on 24 sets of measurements. The average value of 4 replications was used for each set of measurement.

## 3      Results and discussion

The relationship between the vibration amplitude of soldering tool and ultrasonic power as shown in Figure 3 is not proportional but polynomial. Rate of increment in the vibration amplitude values lessened at higher power.



$$y = -0.0246x^2 + 0.825x + 4.3114$$
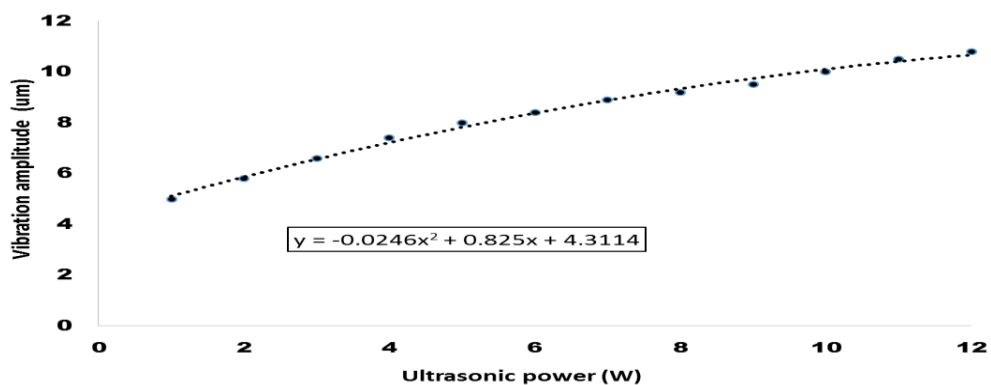
**Figure 3**   Relationship between ultrasonic power and vibration amplitude

| 0.08 μm | 0.15 μm | 0.22 μm |



| 0.26 μm | 0.28 μm | 0.30 μm |
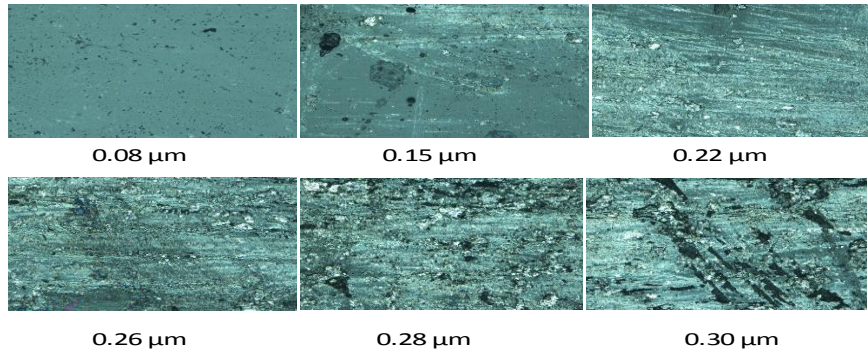
**Figure 4**  Optical microscope sample photos of glass specimen surface roughness

The glass surface roughening produced variable surface roughness Ra ranging from 0.08 to 0.30 μm. The optical microscope sample photos of the selected various surface roughness are shown in Figure 4. Glass surface roughness increased when subjected to both higher vibrational amplitude and longer application time as shown in Figure 5. The surface roughness peaked with power of 10 W and roughening time of 3 - 4 minutes.
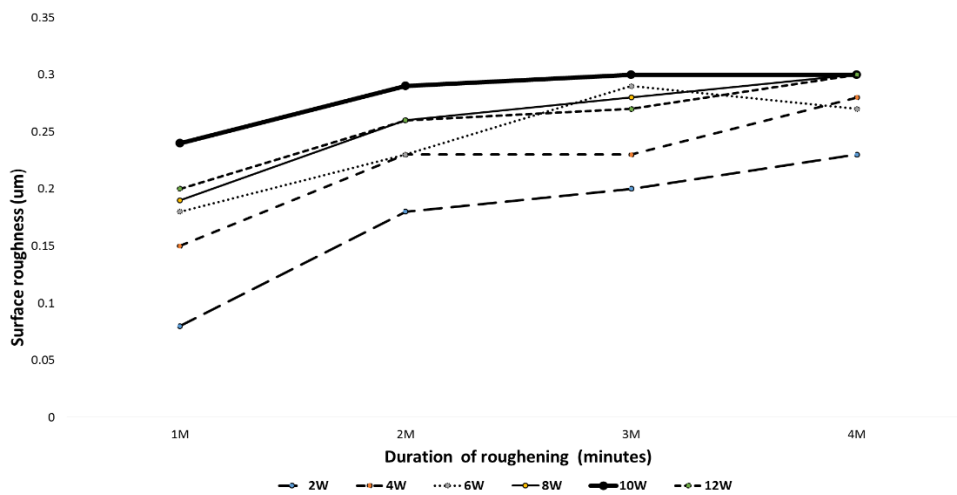


**Figure 5**  Surface roughness against roughening time (Minutes) and vibration amplitude (Watt)
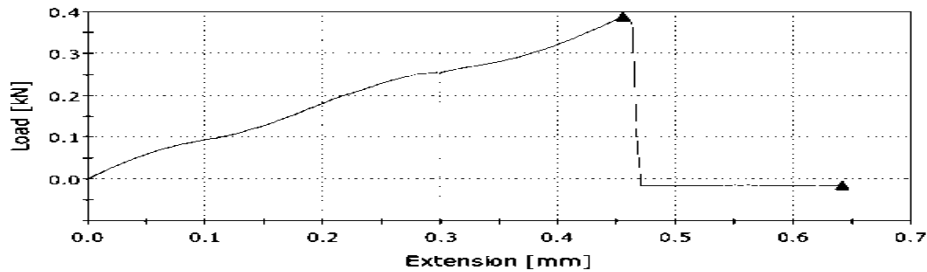
**Figure 6** Graph of shear separation force against the extension before fracture.

Tensile test conducted on the US specimen of glass and Sn5Sb1.2Cu produced the graph of shear separation force and extension before fracture as shown in Figure 6. The relationship between surface roughness and combined data from both shear separation force and solder extension before fracture shear separation force is shown in Figure 7. Shear separation force increased with higher surface roughness values in linear fashion. The rougher surface had larger area compared to smoother surface resulting in larger surface area for surface energy and metal oxide adhesions. In addition, the rougher surface provided greater catchment points for mechanical adhesion of solder to glass.

There is a downward slope of solder extension before fracture with higher surface roughness. High extension values occurred when solders attached to Sn5Sb1.2Cu separated in single piece or completely from glass. At mid Ra ranging from 23-28 µm, separating solders left small patches on glass surface resulting in reduction of extension of solder before fracture values. At higher Ra ranging from 27-30 µm, few glass specimens broke off completely while still attached to solders, resulting in further reduction of solder extension before fracture values. Thus explaining the flattening and stabilizing solder extension values curve at higher surface roughness.
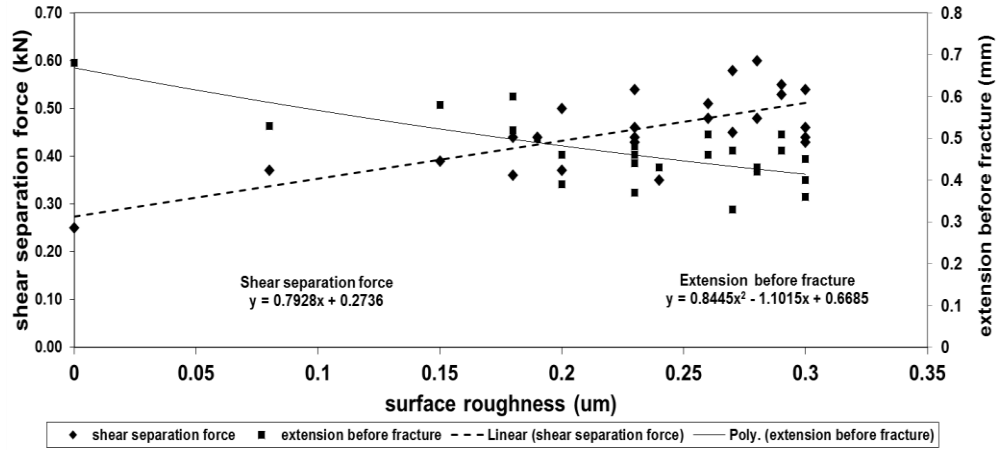
**Figure 7**  Shear separation force and extension before fracture against surface roughness Ra

$$Wsep = (Fn \times Exn \times 0.5)/An \tag{1}$$

Equation for shear separation energy (Wsep) is shown in Equation 1. It is dependent on shear separation force (Fn), extension before fracture (Exn) and surface area (An). The calculated shear separation energy values against surface roughness is shown in Figure 8. The formulation for (Wsep) was obtained using empirical derivation.

$$W_{sep(Sn40Bi)0.5Al} = -2411.1Ra^2 + 1249.9Ra + 733.41 \text{ J/m}^2 \tag{2}$$

Ra is the surface roughness.
Plastic elongation and breakage of solder, deflection and breakage of glass, and deflection of pewter are not taken into account.

The chart shows the equation $y = -2411.1x^2 + 1249.9x + 733.41$
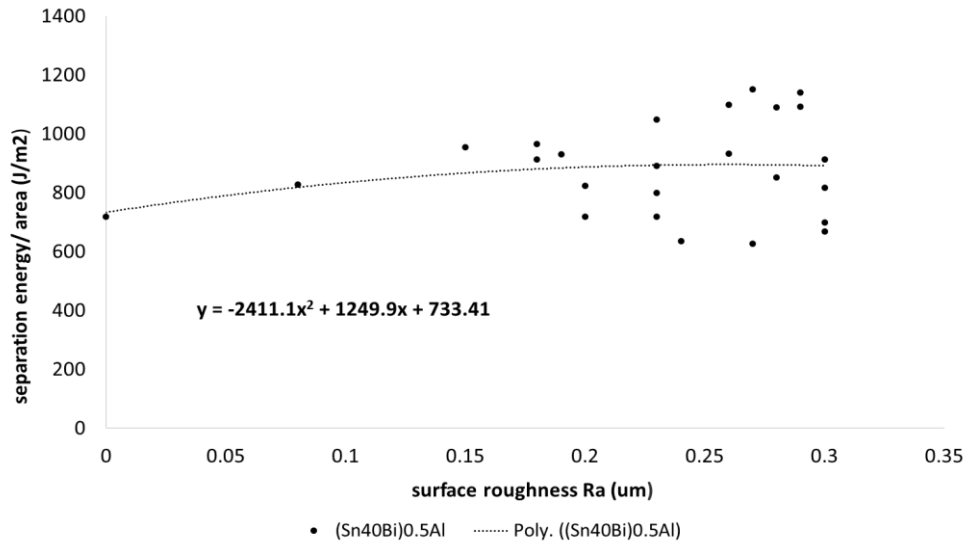
**Figure 8**    Shear separation energy against surface roughness Ra

There is an upward trend of higher shear separation energy with increasing surface roughness. This is due to shear separation force (Fn) being greater with increasing surface Ra. The decreasing values of extension before fracture are not large enough to affect upward slope of shear separation energy until Ra is about 26 μm.  From that point onwards, there is a gentle downward slope. The upward trend of separation energy would continue if not due to solder breakage and glass fracture at higher surface roughness Ra.

The micrograph of the cross section between glass and (Sn40Bi)0.5Al solder joint at Ra of 29 μm using scanning electron microscope (SEM-JEOL JSM-5600) is shown in Figure 9. Bonding of joint between glass and (Sn40Bi)0.5Al solder was through surface energy and metal oxide adhesions. Molten solders also flowed into some crevices creating mechanical adhesion. There were gaps between glass and (Sn40Bi)0.5Al solder signifying incomplete soldering.
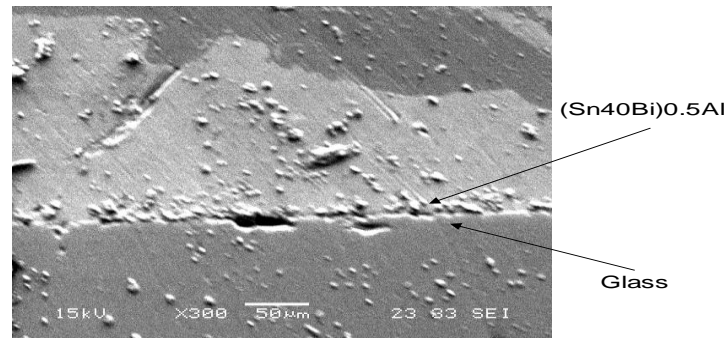
**Figure 9**    SEM micrograph of joint between glass and (Sn40Bi)0.5Al solder

## 4    Conclusion

The effect of glass surface roughness on shear separation energy for US of glass and Sn5Sb1.2Cu using (Sn40Bi)0.5Al solder was studied. Shear separation energy values increased with higher glass surface roughness peaking at Ra 26 µm. Additional surface roughening step was able to increase shear separation energy with uniform energy input as other soldering parameters were kept constant.

## 5    References

[1]    Xu, Z., Ma, L., Yan, J., Yang, S. & Du, S., *Wetting and oxidation during ultrasonic soldering of an alumina reinforced aluminum–copper–magnesium (2024 Al) matrix composite.* Composites: Part A **43**, 407–414, 2012.

[2]    Li, Y.X., Leng, X.S., Cheng, S. & Yan, J.C., *Microstructure design and dissolution behavior between 2024 Al/Sn with the ultrasonic-associated soldering.* Materials and Design **40**. 427–432, 2012.

[3]    Nagaoka, T., Morisada, Y., Fukusumi, M. & Takemoto, T., *Selection of soldering temperature for ultrasonic-assisted soldering of 5056 aluminum alloy using Zn–Al system solders.* Journal of Materials Processing Technology **211**(9) 1534–1539, 2011.

[4]    Nagaoka, T., Morisada, Y., Fukusumi, M. &Takemoto. T., *Ultrasonic-Assisted Soldering of 5056 Aluminum Alloy Using Quasi-Melting Zn-Sn Alloy.* Metallurgical and Materials Transactions B: Process Metallurgy and Materials Processing Science **41** (4), 864-871, 2010.

[5]    Nagaoka, T., Morisada, Y., Fukusumi, M. & Takemoto. T., *Joint strength of aluminum ultrasonic soldered under liquidus temperature of Sn–Zn hypereutectic solder.* Journal of Materials Processing Technology **209** 5054–5059, 2009.

[6]     Li, Y.X., Zhao, W.W., Leng, X.S., Fu, Q.J., Wang, L. & Yan, J.C., *Microstructure evolution and mechanical properties of ultrasonic-assisted soldering joints of 2024 aluminium alloys.* Trans. Non ferrous Met. Soc. China. **2**. 1937 –1943, 2011.

[7]     Ding, M., Zhang P.L., Zhang, Z.Y. & Yao, S., *A novel assembly technology of aluminum alloy honeycomb structure* Int J Adv Manuf Technol **46**:1253– 1258, 2010.

[8]     Kim, W.C., Lee, K.W., Saarinen, I.J., Pykari, L. & Paik, K.W., *Ultrasonic Bonding of Anisotropic Conductive Films Containing Ultrafine Solder Balls for High-Power and High-Reliability Flex-On-Board Assembly* IEEE Transaction on Components, Packaging and Manufacturing Technology, Vol. **2**, No. 5, 2012.

[9]     Lee, K.W., Saarinen, I.J., Pykari, L. & Kyung, W.P., *High Power and High Reliability Flex-On-Board Assembly Using Solder Anisotropic Conductive Films Combined with Ultrasonic Bonding Technique.* IEEE Transaction on Components, Packaging and Manufacturing Technology, Vol. **1**, No. 12. 2011.

[10]    Tamuraa, S., Tsunekawa, Y., Okumiya, M. & Hatakeyama, M., *Ultrasonic cavitation treatment for soldering on Zr-based bulk metallic glass.* Journal of Materials Processing Technology. **206** 322–327, 2008.

[11]    Yamada, M., Nobuhiko, C. & Takayuki. M., *Solder Alloy For Bonding Oxide Material, And Solder Joint Using The Same.* (Patent application number: 20090104071), 2009.

[12]    Finnis, M.W., *The theory of metal–ceramic interfaces* J. Phys.: Condens. Matter **8**: 5811–5836, 1996.